A&A 678, L1 (2023)
https://doi.org/10.1051/0004-6361/202347607

Astronomy & Astrophysics

LETTER TO THE EDITOR

Stability and instability of strange dwarfs

Francesco Di Clemente[1,2], Alessandro Drago[1,2], Prasanta Char[3], and Giuseppe Pagliara[1,2]

[1] Dipartimento di Fisica e Scienze della Terra, Universitá di Ferrara, Via Saragat 1, 44122 Ferrara, Italy
[2] INFN Sezione di Ferrara, Via Saragat 1, 44122 Ferrara, Italy
e-mail: drago@fe.infn.it
[3] Space Sciences, Technologies and Astrophysics Research (STAR) Institute, Université de Liège, Bât. B5a, 4000 Liège, Belgium

Received 30 July 2023 / Accepted 12 September 2023

ABSTRACT

Aims. More than 20 years ago, the existence of stable white dwarfs with a core of strange quark matter was proposed. More recently, via the study of radial modes, it has been concluded instead that such objects are unstable. We aim to clarify this issue.
Methods. We investigated the stability of these objects by looking at their radial oscillations while incorporating boundary conditions at the quark–hadron interface, which correspond to either a rapid or a slow conversion of hadrons into quarks.
Results. Our analysis shows that objects of this type are stable if the star is not strongly perturbed and ordinary matter cannot transform into strange quark matter because of the Coulomb barrier separating the two components. On the other hand, ordinary matter can be transformed into strange quark matter if the star undergoes a violent process, as in the preliminary stages of a type Ia supernova, and this causes the system to become unstable and collapse into a strange quark star. In this way, the accretion-induced collapse of strange dwarfs can be facilitated, and kilometre-sized objects with sub-solar masses can be produced.

Key words. white dwarfs – equation of state – stars: neutron – dark matter

1. Introduction

White dwarfs (WDs) are formed when the progenitor star has a mass below around 9 $M_\odot$ (Heger et al. 2003) and runs out of nuclear fuel at the conclusion of its evolutionary cycle, causing its core to collapse as its outer layers expand. Only when the electrons' degeneracy pressure is sufficient to support the structure does it stop collapsing. Depending on the progenitor mass, the nuclear fusion can lead to the production of different nuclei that correspond to different outcomes of the evolutionary cycle: helium (He) WDs, carbon–oxygen (C–O) WDs, and oxygen–neon–magnesium (O–Ne–Mg) WDs. The maximum mass (Chandrasekhar mass) of WDs is about 1.4 $M_\odot$ (Chandrasekhar 1931), depending on their composition, and most of them are C–O WDs.

In 1995 it was proposed that WDs can harbour a core of absolutely stable strange quark matter (satisfying the Bodmer–Witten hypothesis; Bodmer 1971; Witten 1984) at their centre and that the presence of this strange core can stabilize objects that otherwise would be unstable (Glendenning et al. 1995a,b). These objects, called strange dwarfs (SDs), can have radii, masses, and an astrophysical evolution that is different from those of normal WDs (Glendenning et al. 1995a,b; Alford et al. 2017). It was suggested that they form either by cumulating normal nuclear matter on the surface of a strange quark star (QS) or from WDs collecting nuggets of strange quark matter (strangelets) already present in the Galaxy. Glendenning et al. (1995a) discussed the radial stability of SDs and show that they can be stable for nuclear matter envelope densities far exceeding the maximum densities of WDs.

The question of the stability of SDs was reconsidered in Alford et al. (2017), who show that the eigenvalue of the fundamental radial mode is negative, indicating that such systems are unstable[1]. Since the two calculations seemed to be based on the same hypothesis, the problem remained unsettled.

In this Letter we reconsider the stability of SDs by discussing an aspect that was not investigated in the previous papers, that is, the appropriate boundary conditions at the interface between nuclear matter and the quark core. In this analysis we use the formalism developed in Pereira et al. (2018) and Di Clemente et al. (2020), who show that different boundary conditions need to be applied depending on the rapidity of the conversion of nuclear matter into quark matter and that those boundary conditions can modify the eigenvalue of the radial oscillations and, therefore, the stability of the star. We also show how the traditional stability criterion based on counting the extrema in the mass–radius (MR) plane (Zel'dovich 1963; Bardeen et al. 1966) remains valid but that it must be implemented by explicitly specifying if, during the radial oscillation, the quark content is kept constant or not.

Finally, the results of our analysis prove to be relevant when discussing the accretion-induced collapse (AIC) of WDs (Canal et al. 1990) and the possibility of kilometre-sized objects of sub-solar mass forming, such as SAX J1808.4−3658 (Di Salvo et al. 2019)[2].

[1] In Alford et al. (2017), it was suggested that Glendenning et al. (1995a,b) mistook the second-lowest eigenmode for the lowest one.
[2] It has recently been proposed that the central compact object associated with HESS J1731−347 also has a small radius and a sub-solar mass (Doroshenko et al. 2022). Our analysis suggests that the object is also a QS (Di Clemente et al. 2022).

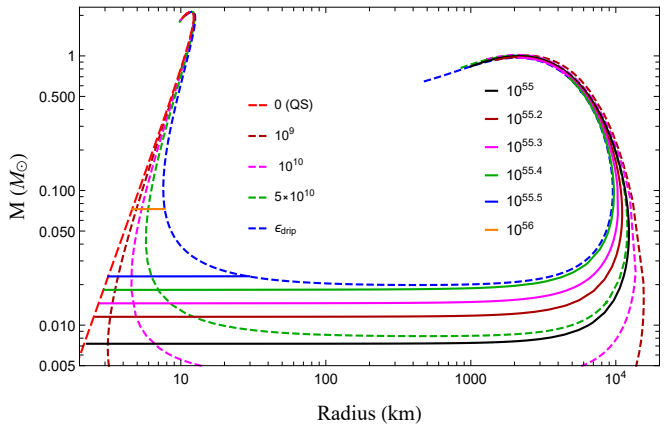

Fig. 1. MR sequences. Dashed lines show configurations in which P_t is constant. Values of P_0 (and therefore also B_{core}) increase clockwise. The legend indicates ε_t values in g cm^{-3}. Solid lines show configurations in which B_{core} is constant. Here, P_0 (and therefore also P_t) increases in the anti-clockwise direction. The legend indicates the value of B_{core}.

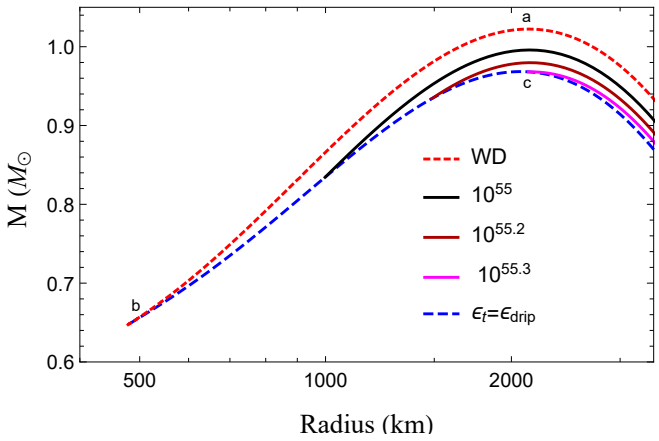

Fig. 2. Magnification of the MR sequence close to the Chandrasekhar limit. The notation is the same as in Fig. 1. The WD configuration (not shown in Fig. 1) is also displayed.

2. Structure of strange dwarfs

What allows SDs to form is, crucially, that nuclear matter is separated from the core of quark matter by a Coulomb barrier as long as the maximum density of nuclear matter, ε_t, is smaller than the neutron drip density, $\varepsilon_{drip} \sim 4\times10^{11}$ g cm^{-3}. This is what allows SDs to form. Above ε_{drip} free neutrons are present and, since they are not influenced by the Coulomb barrier, they fall into the quark matter core, where they are rapidly absorbed and their quarks deconfined.

The equation of state (EoS) describing this situation and used in Glendenning et al. (1995a,b) reads

$$\varepsilon(P) = \begin{cases} \varepsilon_{BPS}(P) & P \le P_t \\ \varepsilon_{quark}(P) & P > P_t \end{cases}, \tag{1}$$

where ε_{BPS} is the Baym–Pethick–Sutherland (BPS) EoS (Baym et al. 1971) and ε_{quark} is an EoS for the strange quark matter (e.g., one based on the MIT bag model[3]). The transition pressure $P_t \equiv P(R_{core}) = P(\varepsilon = \varepsilon_t)$ is the pressure at the radius of the interface separating quarks and nuclear matter. We note that the BPS EoS provides a Chandrasekhar mass of about 1 $M_\odot$.

Any value of ε_t can be used as long as $\varepsilon_t < \varepsilon_{drip}$. This implies that to define a specific SD stellar configuration, obtained by solving the Tolman–Oppenheimer–Volkoff (TOV) equation (Oppenheimer & Volkoff 1939), one has to define two parameters: P_t and the central pressure of the star, $P_0 \equiv P(r = 0) = P(\varepsilon_0)$. This difference with respect to the case for normal WDs plays an important role in the discussion of the stability.

Since the solutions of the TOV equation for SDs are bi-parametric, one has to consider whether the choice of the pair of parameters (P_0, P_t) is the most appropriate. As discussed in a series of papers by Vartanyan et al. (2009, 2012), as long as nuclear matter cannot transform into quark matter, one can define sequences of configurations with the same quark baryon number, B_{core}, and, therefore, choose the two parameters to be (P_0, B_{core}). The quark baryon number reads

$$B_{core}(\varepsilon_0, \varepsilon_t) = \int_0^{R_{core}} 4\pi r^2 \frac{\rho(r)}{\sqrt{1-2m(r)/r}}\,dr, \tag{2}$$

where ρ is the baryon density. It should be noted that the two choices are not equivalent because if one keeps P_t constant, then B_{core} changes with P_0, describing a situation in which hadrons can deconfine into quarks. If instead B_{core} is kept constant, then P_t must increase with increasing P_0, describing a situation in which hadrons cumulate on the surface of the strange core without being absorbed.

While it is straightforward to build sequences of solutions of the TOV equation obtained by keeping P_t constant and varying P_0, it is numerically more cumbersome to produce sequences of solutions specified by a given value of B_{core}. The reason is that Eq. (2) provides B_{core} as a function of (P_0, P_t), but the inverse relation, providing P_t as a function of (P_0, B_{core}), can only be obtained numerically[4].

In Fig. 1 we show the MR relations obtained by keeping either P_t or B_{core} fixed. If B_{core} = constant, the configurations with smaller P_0 values are at the left of the diagram (QSs without any nuclear matter mantle, i.e., $\varepsilon_t = 0$). These pure QS configurations have no unstable mode. With increasing P_0, we move anti-clockwise and, according to the general stability criterion (Zel'dovich 1963; Bardeen et al. 1966), the configurations remain stable until they reach the maximum mass, at which the fundamental mode becomes unstable (which happens for $B_{core} \lesssim 10^{55.3}$), or until they reach $\varepsilon_t = \varepsilon_{drip}$ (if $B_{core} \gtrsim 10^{55.3}$), as discussed in Glendenning et al. (1995a,b) and Vartanyan et al. (2009, 2012). Above that value of ε_t, free neutrons are produced, and the configuration is no longer stable.

Instead, if P_t is kept constant, we start from the top-right, purely nucleonic WD configurations in which $B_{core} = 0$ (completely stable WD configurations to the right of point a in Fig. 2). By increasing P_0, we reach point a, where the fundamental mode becomes unstable. By further increasing P_0, we reach P_t, at which quarks start being present, and the curve displays a turning point (point b in Fig. 2 if $\varepsilon_t = \varepsilon_{drip}$). At point b the first excited mode also becomes unstable (the path until b is followed in an anti-clockwise direction). At (c) (this extreme point is reached moving clockwise), the first excited mode again

[3] The thermodynamic potential of the bag model reads $\Omega(\mu) = -\frac{3}{4\pi^2}a_4\mu^4 + \frac{3}{4\pi^2}(m_s^2 - 4\Delta_0^2)\mu^2 + B$. In our calculations, we used $a_4 = 1$, gap parameter $\Delta_0 = 10$ MeV, strange quark mass $m_s = 120$ MeV, and bag constant $B = 135^4$ MeV^4.

[4] To this purpose, we found the following expansion useful: $\varepsilon_0(B_{core}, \varepsilon_t) \simeq \varepsilon_t^Q/[1 - k_1\,\varepsilon_t^Q\,B_{core}^{2/3} - k_2\,(\varepsilon_t^Q)^2\,B_{core}^{4/3}]$, where $\varepsilon_t^Q = \varepsilon_{quark}(P_t(\varepsilon_t))$ and k_1, k_2 are parameters determined by numerically inverting Eq. (2). Notice that as long as the quark core is small, $\varepsilon_0 \sim \varepsilon_t^Q$, but the difference between these two energy densities is crucial for obtaining the correct solutions.

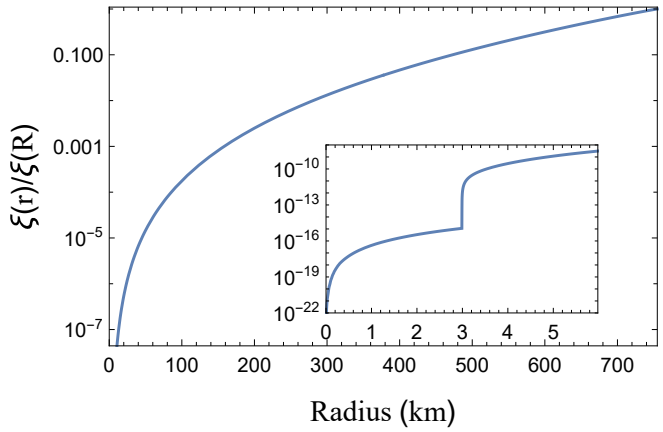

Fig. 3. Fundamental eigenfunction of radial modes in the slow scenario in which hadrons do not deconfine into quarks during the oscillation timescale. The star considered here and in Fig. 4 has $M \simeq 0.02\,M_\odot$, $B_{\rm core} \simeq 2.69 \times 10^{55}$, and $\varepsilon_{\rm t} = \varepsilon_{\rm drip}$ and is located to the right of the minimum of the dashed blue curve in Fig. 1. Here, the mode is stable: $\omega^2 = 0.788275\,{\rm Hz}^2$. In the inset plot, the region around $r = r_{\rm t}$ is magnified: there the eigenfunction has a kink.

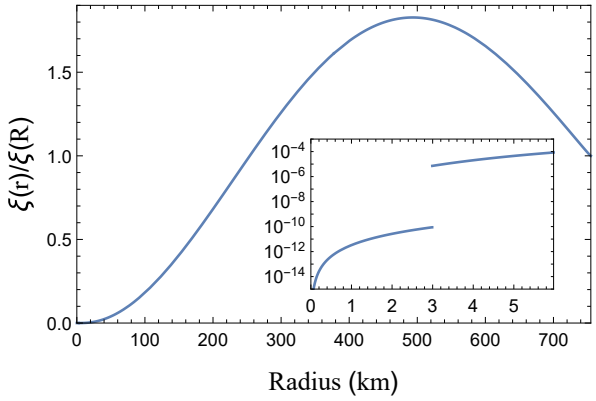

Fig. 4. Fundamental eigenfunction in the case of rapid transitions, similar to the scenario discussed in Alford et al. (2017). Here, the mode is unstable, $\omega^2 = -1.62785\,{\rm Hz}^2$, and the eigenfunction is discontinuous.

becomes stable but the fundamental mode remains unstable until the minimum mass is reached at a radius of a few hundred kilometres, as discussed in Alford et al. (2017). In conclusion, in both cases the general stability criterion of Zel'dovich (1963) and Bardeen et al. (1966) is satisfied.

In Fig. 2 we show that, as suggested in Glendenning et al. (1995a,b), there are indeed stable configurations of SDs in which the largest density of nuclear matter exceeds that reached in normal WDs. Nevertheless, we note that these configurations are reached only if $B_{\rm core} \gtrsim 10^{52}$ (see Fig. 6); otherwise, the structure of an SD with $M \sim M_\odot$ is very similar to that of a WD. Another important difference between the structure of SDs and WDs concerns objects with $M \lesssim 0.1\,M_\odot$: their radius can be significantly smaller than that of a WD; the existence of this type of object has been recently suggested in Kurban et al. (2022).

3. Radial oscillations

To check the stability of a configuration, we studied radial oscillations. Schwarzschild's line element for a non-rotating symmetric star reads

$$ds^2 = e^{2\phi}dt^2 - e^{2\lambda}dr^2 - r^2(d\theta^2 + \sin^2\theta d\phi^2), \tag{3}$$

where $\phi \equiv \phi(r)$ and $\lambda \equiv \lambda(r)$ are the metric potentials. Using this metric, the differential equation for radial oscillations reads

$$(H\xi')' = -(\omega^2 W + Q)\xi, \tag{4}$$

where $\xi(r)$ is the Lagrangian displacement multiplied by $r^2 e^{-\phi}$ and ω is the characteristic frequency of the mode. Here,

$$\begin{aligned} H &= r^{-2}(\varepsilon + P)e^{\lambda+3\phi}c_{\rm s}^2 \\ Q &= r^{-2}(\varepsilon + P)e^{\lambda+3\phi}(\phi'^2 + 4r^{-1}\phi' - 8\pi e^{2\lambda}P) \\ W &= r^{-2}(\varepsilon + P)e^{3\lambda+\phi}, \end{aligned} \tag{5}$$

where $c_{\rm s}^2$ is the sound velocity. The important point is that when multiple layers or phase transitions are present, one has to specify boundary conditions on the separating surfaces, as discussed in Pereira et al. (2018) and Di Clemente et al. (2020). In particular, one has to clarify if, during the timescale of the oscillation, the two components of the fluid can transform from one into the other. We are now going to discuss these two possibilities.

Slow transition. The slow phase transition scenario occurs when the characteristic timescale of the conversion of one phase into the other is much longer than that of the perturbation. The two phases do not mix, and the volume element close to the surface separating the two phases moves with the interface, expanding and contracting. This case applies to SDs in which $\varepsilon_{\rm t} < \varepsilon_{\rm drip}$, and it corresponds in the MR diagram to sequences of configurations in which $B_{\rm core}$ is kept constant.

The interface conditions for the slow conversion are the continuity of the radial displacement at $r_{\rm t}$,

$$[\xi]^+_- \equiv \xi(r_{\rm t}^+) - \xi(r_{\rm t}^-) = 0, \tag{6}$$

and the continuity of the Lagrangian perturbation of the pressure,

$$[\Delta P]^+_- = \left[-e^{\phi}\, r^{-2}\, \gamma(r)\, P\, \frac{\partial \xi}{\partial r}\right]^+_- = 0, \tag{7}$$

where $\gamma(r) = (\partial P/\partial\varepsilon)(\varepsilon + P)P^{-1}$ is the relativistic adiabatic index. By solving Eq. (4) with conditions (6) and (7), we obtain that $\omega^2 > 0$, and it vanishes at the maximum mass in the MR plane along the curve obtained by keeping $B_{\rm core}$ constant, as suggested by the Zel'dovich (1963) and Bardeen et al. (1966) criterion. The eigenfunctions are continuous and have a kink at $r_{\rm t}$ (see Fig. 3), and the same behaviour is displayed by $\Delta P(r)$.

Rapid transition. When the timescale of the conversion of the two phases is shorter than that of the perturbation, mass transfer between the two phases is possible. The surface separating the two phases is in thermodynamic equilibrium since the conversion rates are very rapid; therefore, Eq. (7) also applies to this case. The only difference with the slow transition case is that the interface condition in Eq. (6) becomes

$$\left[\xi + \frac{\gamma P \xi'}{P'}\right]^+_- = 0, \tag{8}$$

such that the eigenfunction has a discontinuity at the interface.

The origin of the apparent discrepancy between the results of Glendenning et al. (1995a,b) and those of Alford et al. (2017) is now clear. In Alford et al. (2017), the used EoS is similar to the one discussed in Eq. (1), but a smoothing is introduced[5]

[5] The smoothed EoS used in Alford et al. (2017) reads $\varepsilon(P) = [1 - \tanh((P - P_{\rm crit})/\delta P)\,\varepsilon_{\rm BPS}(P)]/2 + [1 + \tanh((P - P_{\rm crit})/\delta P)\,\varepsilon_{\rm quark}(P)]/2$, where δP is the transition width.

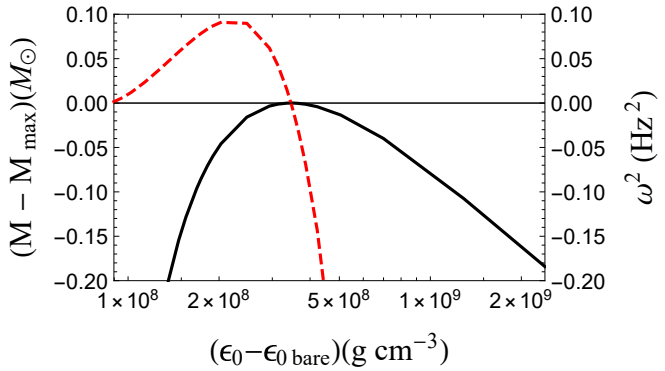

Fig. 5. Eigenvalues of the fundamental mode in the slow case (dashed) and masses of SDs with $B_{\rm core} = 10^{55}$, close to the maximum, $M_{\rm max} \sim 0.996\,M_\odot$ (solid), plotted as functions of the central energy density, ϵ_0. The zero of ω^2 coincides with the maximum mass, and it turns negative at higher densities. Since ϵ_0 remains almost constant in the range displayed in the figure, we show its tiny change with respect to the central density, $\epsilon_{0\ \rm bare}$, of a pure QS that has the same $B_{\rm core}$.

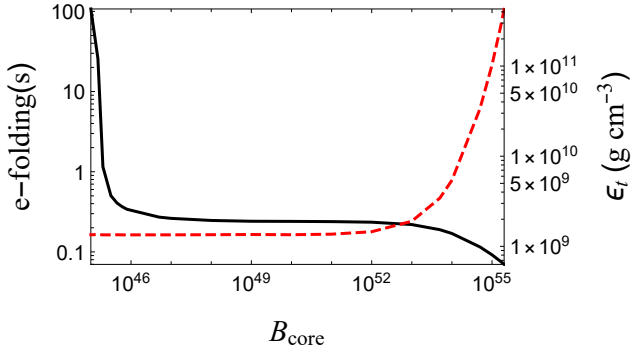

Fig. 6. Properties of maximum mass stars as a function of their quark content. The solid black line shows the timescale of the mechanical instability as a function of $B_{\rm core}$. The dashed red line shows the transition density.

so that there is no sharp discontinuity between the two phases and, crucially, they can transform instantaneously from one into the other. This is similar to the rapid case discussed in this Letter: while in Alford et al. (2017) the eigenfunction does not display a discontinuity at the interface, a very fast increase in its value takes place, the size of which is totally equivalent to that displayed in our Fig. 4. On the other hand, no discussion on the boundary conditions at the interface is presented in Glendenning et al. (1995a,b), but most likely the eigenfunction was assumed to be continuous, which is the situation described in our slow scenario.

The distinction between slow and rapid processes was already introduced in the 1960s (see e.g., Thorne 1966), when it was noted that the agreement between the stability analysis based on the solutions of the TOV equation (static analysis) and that based on the study of the radial oscillation equation (dynamic analysis) depends on the use in the eigenvalue equation of an adiabatic index that is derived from the EoS adopted in the static analysis. It is easy to satisfy this agreement in the rapid case. It is, in general, far from easy in the slow case because the slow adiabatic index is computed by taking imbalances produced by the perturbation into account (Lindblom & Owen 2002; Drago et al. 2005), while an imbalanced EoS is generally not introduced. Our case is particularly straightforward because the conversion between hadrons and quarks can take place only on a bi-dimensional surface (and not over an extended volume). It is, therefore, easy to modify both the adiabatic index (this corresponds to modifying the interface conditions; Pereira et al. 2018) and the EoS (the slow case corresponds to keeping the quark content completely frozen; Vartanyan et al. 2009, 2012). In this way, we also have a correspondence between static and dynamic analyses in the slow case, as shown in Fig. 5 (in the rapid case this was already proven by Alford et al. 2017).

4. Implications for SD collapse

The presence of a strange quark matter core in SDs can play a crucial role when the object is strongly perturbed, as occurs in the preliminary stages of a type Ia supernova. In particular, it can help the object collapse instead of following the path that leads to a deflagration. The difficulty in producing an AIC in a WD is due to the fact that strong nuclear reactions start taking place when the star is close to the Chandrasekhar limit, that is, in a situation in which the star is still marginally mechanically stable ($\omega^2 \simeq 0$), and they disrupt the star before AIC takes place (Canal et al. 1990). We have shown in this Letter that the mechanical stability in the case of SDs depends on the possibility of hadrons rapidly converting into quarks. As long as $\varepsilon_{\rm t} \ll \varepsilon_{\rm drip}$, the object is mechanically stable, but if a fluctuation produces matter at densities above $\varepsilon_{\rm drip}$, the system becomes unstable. We can estimate this instability by computing the fundamental eigenvalue of a star at the Chandrasekhar limit along a line where $B_{\rm core}$ is constant. In the case of a slow transition, $\omega^2 = 0$; however, in the case of a rapid transition, ω^2 is large and negative. In Fig. 6 we show the e-folding time $= 2\pi/|\omega|$; we can see here that for $B_{\rm core} \gtrsim 10^{46}$ the typical time of growth of the instability drops well below $1\,s$, suggesting that the collapse can be faster than the development of the deflagration (Gamezo et al. 2003)[6]. In the same figure we also show $\varepsilon_{\rm t}$, the maximum density reached by the nuclear matter component. As anticipated earlier, the static structure of an SD with $M \sim M_\odot$ does not change until $B_{\rm core} \gtrsim 10^{52}$. For smaller values of $B_{\rm core}$, $\varepsilon_{\rm t}$ equals the central density of a WD, indicating that the quark core affects the stability of the star for values of $B_{\rm core}$ smaller than those needed to affect its static properties.

A very important question concerning SDs is how they can collect the strange quark matter sitting at their centre. The most obvious answer is that WDs accumulate strangelets during their lifetime. To this purpose, the formula of Madsen (1988) is very useful: it indicates the rate of strangelets hitting the surface of a star of mass M and radius R. If we assume that dark matter is made of strangelets[7] with a density equal to that of dark matter in the galactic halo, $\rho_{\rm DM} \sim 10^{-24}\,{\rm g\,cm^{-3}}$, and a velocity of $250\,{\rm km\,s^{-1}}$, the rate reads

$$F \sim (1.39 \times 10^{30}\ {\rm s^{-1}}) A^{-1} (M/M_\odot)(R/R_\odot). \quad (9)$$

A WD close to the Chandrasekhar mass with a radius of $\sim$3000 km can in 5 Gy reach $B_{\rm core} \sim 10^{45}$, just slightly smaller than the size needed to affect the dynamics of AIC. We can

[6] We also computed the e-folding time for a different set of parameters for the quark EoS, i.e., those in Bombaci et al. (2021). The results are unchanged.

[7] The possibility that dark matter is made of strangelets has been discussed in a few recent papers (Burdin et al. 2015; Jacobs et al. 2015; Caloni et al. 2021), and the search for these objects is at the core of many observation campaigns (Bacholle et al. 2021; Olinto 2021; Casolino et al. 2015).

nonetheless see that the density distribution of dark matter grows rapidly towards the centre (see for example Navarro et al. 1997), meaning that in the most central regions of the Milky Way, $B_{\rm core}$ can easily be large enough to favour AIC. This can be useful to justify schemes in which it is assumed that the AIC is very common close to the galactic centre, such as in the scenario developed to interpret the gamma-ray excess signal from the galactic centre (Gautam et al. 2022).

It is interesting to compare the scenario we are describing with the one proposed in Leung et al. (2013), where the impact of dark matter on the AIC of WDs is also discussed. The main difference is that in Leung et al. (2013) dark matter and normal matter cannot transform into each other (which is the cause of the instability described in this Letter) and, therefore, a huge amount of dark matter is needed to affect the structure of the WD only through gravity. This is consistent with our Fig. 6, where we show that a core of strange quark matter can destabilize the star (by mixing with ordinary matter) even if its size is much smaller than that needed to influence the structure of the star through gravity. In this way, AIC is facilitated and requires an amount of strange quark matter totally compatible with the density of dark matter in our galaxy, as discussed above.

Another interesting outcome of the AIC of SDs is the possibility of producing kilometre-sized objects with sub-solar masses. We note that the outcome of an AIC of an SD is a QS and not a neutron star because the large core of strange quark matter would rapidly transform nucleons into quarks (Drago & Pagliara 2015). In order to estimate the mass of the object produced after the collapse, we must first note that in our calculation we have used the BPS EoS for the sake of simplicity, but a more realistic calculation based on a C–O WD would give a Chandrasekhar mass of $\sim 1.4\,M_{\odot}$. In the case of an AIC of a WD into a neutron star, the extra binding in the more compact object corresponds to roughly $0.1\,M_{\odot}$, but if a QS forms from an SD, its gravitational mass can be lower than $\sim 1.1\,M_{\odot}$ (Bombaci et al. 2021). Moreover, the huge amount of energy released in the conversion can increase the amount of mass ejected during the AIC (Sharon & Kushnir 2020), so the final configuration can be a QS with a radius $R \lesssim 11$ km and a mass lower than that of the Sun. It is worth noting that SAX J1808.4−3658 is reported to have a small radius (Li et al. 1999; Poutanen & Gierlinski 2003; Leahy et al. 2008), an accelerated cooling (Heinke et al. 2009), and a sub-solar mass (Di Salvo et al. 2019), all features suggesting that it is a QS, possibly produced through an AIC of an SD.

Acknowledgements. We thank Michał Bejger for several useful discussions during the preparation of this work. P.C. is currently supported by the Fonds de la Recherche Scientifique-FNRS, Belgium, under grant No. 4.4503.19.

References

Alford, M. G., Harris, S. P., & Sachdeva, P. S. 2017, ApJ, 847, 109
Bacholle, S., Barrillon, P., Battisti, M., et al. 2021, ApJS, 253, 36
Bardeen, J. M., Thorne, K. S., & Meltzer, D. W. 1966, ApJ, 145, 505
Baym, G., Pethick, C., & Sutherland, P. 1971, ApJ, 170, 299
Bodmer, A. R. 1971, Phys. Rev. D, 4, 1601
Bombaci, I., Drago, A., Logoteta, D., Pagliara, G., & Vidaña, I. 2021, Phys. Rev. Lett., 126, 162702
Burdin, S., Fairbairn, M., Mermod, P., et al. 2015, Phys. Rept., 582, 1
Caloni, L., Gerbino, M., & Lattanzi, M. 2021, J. Cosmol. Astropart. Phys., 07, 027
Canal, R., Isern, J., & Labay, J. 1990, ARA&A, 28, 183
Casolino, M., Farooque, T., Juste, A., et al. 2015, Exp. Astron., 40, 19
Chandrasekhar, S. 1931, ApJ, 74, 81
Di Clemente, F., Mannarelli, M., & Tonelli, F. 2020, Phys. Rev. D, 101, 103003
Di Clemente, F., Drago, A., & Pagliara, G. 2022, ArXiv e-prints [arXiv:2211.07485]
Di Salvo, T., Sanna, A., Burderi, L., et al. 2019, MNRAS, 483, 767
Doroshenko, V., Suleimanov, V., Puehlhofer, G., & Santangelo, A. 2022, Nat. Astron., 6, 1444
Drago, A., & Pagliara, G. 2015, Phys. Rev. C, 92, 045801
Drago, A., Lavagno, A., & Pagliara, G. 2005, Phys. Rev. D, 71, 103004
Gamezo, V. N., Khokhlov, A. M., Oran, E. S., Chtchelkanova, A. Y., & Rosenberg, R. O. 2003, Science, 299, 77
Gautam, A., Crocker, R. M., Ferrario, L., et al. 2022, Nat. Astron., 6, 703
Glendenning, N. K., Kettner, C., & Weber, F. 1995a, Phys. Rev. Lett., 74, 3519
Glendenning, N. K., Kettner, C., & Weber, F. 1995b, ApJ, 450, 253
Heger, A., Fryer, C. L., Woosley, S. E., Langer, N., & Hartmann, D. H. 2003, ApJ, 591, 288
Heinke, C. O., Jonker, P. G., Wijnands, R., Deloye, C. J., & Taam, R. E. 2009, ApJ, 691, 1035
Jacobs, D. M., Starkman, G. D., & Lynn, B. W. 2015, MNRAS, 450, 3418
Kurban, A., Huang, Y.-F., Geng, J.-J., & Zong, H.-S. 2022, Phys. Lett. B, 832, 137204
Leahy, D. A., Morsink, S. M., & Cadeau, C. 2008, ApJ, 672, 1119
Leung, S. C., Chu, M. C., Lin, L. M., & Wong, K. W. 2013, Phys. Rev. D, 87, 123506
Li, X. D., Bombaci, I., Dey, M., Dey, J., & van den Heuvel, E. P. J. 1999, Phys. Rev. Lett., 83, 3776
Lindblom, L., & Owen, B. J. 2002, Phys. Rev. D, 65, 063006
Madsen, J. 1988, Phys. Rev. Lett., 61, 2909
Navarro, J. F., Frenk, C. S., & White, S. D. M. 1997, ApJ, 490, 493
Olinto, A. V., et al. 2021, J. Cosmol. Astropart. Phys., 06, 007
Oppenheimer, J. R., & Volkoff, G. M. 1939, Phys. Rev., 55, 374
Pereira, J. P., Flores, C. V., & Lugones, G. 2018, ApJ, 860, 12
Poutanen, J., & Gierlinski, M. 2003, MNRAS, 343, 1301
Sharon, A., & Kushnir, D. 2020, ApJ, 894, 146
Thorne, K. S. 1966, in The General-Relativistic Theory of Stellar Structure and Dynamics, (New York: Academic Press), Proceedings of the International School of Physics Enrico Fermi. Course XXXV, at Varenna, Italy, July 12–24, 166
Vartanyan, Y. L., Hajyan, G. S., Grigoryan, A. K., & Sarkisyan, T. R. 2009, Astrophysics, 52, 300
Vartanyan, Y. L., Hajyan, G. S., Grigoryan, A. K., & Sarkisyan, T. R. 2012, Astrophysics, 55, 98
Witten, E. 1984, Phys. Rev. D, 30, 272
Zel'dovich, Y. B. 1963, Voprosy kosmogonii, 9, 36